Divyabharathi et al. 2018. *Int. J. Vehicle Structures & Systems*, 10(1), 14-17
ISSN: 0975-3060 (Print), 0975-3540 (Online)
doi:10.4273/ijvss.10.1.04

International Journal of Vehicle Structures & Systems
Available online at www.maftree.org/eja

Performance of Circular to Non Circular Shape Scramjet Isolators

P. Divyabarathi[a,c], D. Anand[a], S.P. Richards[a] and D.S. Chand[b]

[a]*Dept. of Aeronautical Engg., Bharath Institute of Higher Education and Research, Chennai, India*
[b]*Dept. of Aeronautical Engg., Tagore Engg. College, Chennai, India*
[c]*Corresponding Author, Email: divyabarathi.aero@bharathuniv.ac.in*

ABSTRACT:

This paper details the influence of geometry variation such as shape transition of the isolator from its entry to exit on overall performance of scramjet isolators. The experiments are conducted to assess the performance of two isolator geometries of circle to pentagon and circle to hexagon. The pseudo shock length is obtained for the two cases by observing the sudden pressure rise in pressure plots taken along the wall. It is found that the shock train length is shorter for circular to pentagon duct compared with the other duct. Hence, this duct is preferable in order to prevent inlet non-start induced by the pressure rise in the combustion chamber.

KEYWORDS:

Scramjet isolator; Shape; Shock train; Pressure; Performance; Efficiency

CITATION:

P. Divyabharathi, D. Anand and S.P. Richards and D.S. Chand. 2018. Performance of Circular to Non Circular Shape Scramjet Isolators, *Int. J. Vehicle Structures & Systems*, 10(1), 14-17. doi:10.4273/ijvss.10.1.04.

1. Introduction

A scramjet (supersonic combustion ramjet) is a variation of a ramjet air breathing combustion in jet engine in which the combustion process takes place in supersonic airflow. A scramjet relies on high vehicle speed to powerfully compress in addition to decelerate the incoming air before combustion. The top speed of a scramjet is between Mach 12 and Mach 24 [1]. The scramjet consists of a converging inlet, combustor and diverging nozzle. Very few moving parts are needed in a scramjet, which greatly simplifies both the design and operation of the engine [2]. The isolator lies between the inlet and combustion chamber in an air breathing supersonic/ hypersonic dual mode scramjet engine. The isolator serves two purposes, the first is to isolate the inlet from disturbances in the combustor and the second is to provide the shock train with enough duct length to develop and allow as much pressure increase as possible between the inlet and the combustor based on the given isolator length. The maximum amount of pressure increase in an isolator is equal to that across a normal shock, but this increase is, instead, spread across the length of a shock train, the composition of which is either a series of λ-type shocks or oblique shocks [3].

The studies [3-5] on a supersonic-exit isolator which has series of oblique shock waves have been conducted lately because of the limited resources of the experimental equipment, computer performance, and knowledge of supersonic internal flow. Concerning subsonic-exit isolators, experimental researches [5] were performed to comprehend the flow-structure including a λ-type shock wave and X-type shock wave, and to demonstrate the effects of geometry. Furthermore, theoretical diffusion model, modified diffusion model and mass-averaging pseudo-shock model were proposed to predict the flow properties inside an isolator.

2. Experimental methodology

The behaviour of square isolator configuration under adverse pressure gradient is chosen for experimental study [5]. The experimental study allows real time analysis and can also be used to validate the numerical results. The experiment is conducted in the jet facility (see Fig. 1) laboratory at Bharath University. The experiment was carried out by controlling the nozzle inlet total pressure from 400 kPa to 600 kPa. This reduction in total pressure increases the isolator pressure ratio. Therefore, in experimental work the back pressure imposed is the constant atmospheric pressure where different back pressures are imposed with the same inlet conditions. The isolator wall pressure is measured during experiment using manometer. The manometer has 1 (one) channel and measures the pressure values simultaneously using the channel pressure sensors.

Fig. 1: Jet facility at Bharath University

The isolator duct is of cuboid volume with circular to pentagon cross section of dimension 78.5 mm^2 maintained across its length. The length of the isolator is 100 mm. Hence, the aspect ratio of the isolator (L/D) is

10. The isolator is designed with mild steel EN8 walls which has slots to house the rubber sheet windows which act as side walls. The center line of bottom wall is drilled with holes of 1 mm diameter to measure the wall static pressure. A total of 9 such holes are drilled in the interval of 10 mm to enable the measurement of wall pressure along the isolator length. The front and rear portion of this steel-rubber housing is closed with mild steel flanges of 5 mm thickness. The flanges also have circular pockets of isolator entry dimensions, thus the overall length of the isolator is 100 mm. The designed isolators are shown in Fig. 2 and Fig. 3. The isolator has 9 pressure tappings. The tappings near the isolator exit are covered for lower pressure ratios. As the shock train is positioned near the exit, the tappings in the isolator's mid region and entrance are covered for higher pressure ratios. The unused pressure tappings are sealed during experiment run to avoid bleed. The experimental set-up consists of compressor, storage tank, flow control valve, settling chamber, pressure regulator, convergent – divergent nozzle and isolator duct. For each total pressure setting, the experiment run is executed several times in order to ensure consistency in pressure measurement data.

Fig. 2: Pentagon (left) &Hexagon (right) isolator exit

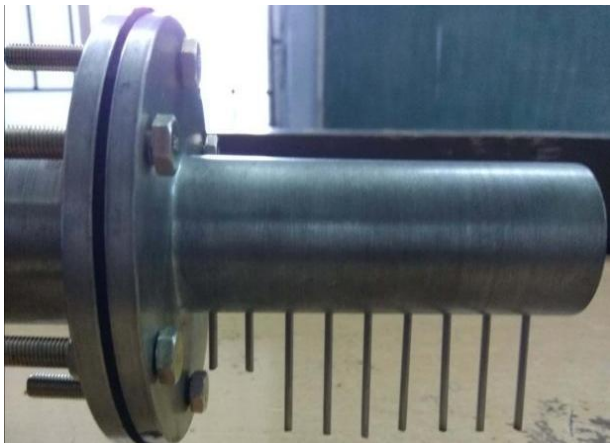

Fig. 3: Isolator with pressure tappings

3. Results and discussion

The static pressure over the isolator wall is measured with scanner for the considered 3 total pressure setups. Each inlet condition is experimented for 3 to 4 times to ensure a consistency in pressure data measurements. For the pentagon shaped exit, Figs. 4 to 6 show the variation of P/P_0 over X/D for total pressure of 400 kPa, 500 kPa and 600 kPa respectively. For 400 kPa setup and at X/D = 0.1, the wall pressure is 0.26 of the total pressure. It is observed that up to X/D = 0.4 the wall pressure increases linearly to a value of 0.2475 for P_0. From X/D = 0.4 to 0.6, the slope of wall pressure is steeper, which is a clear indication of rise in pressure. It may be due to presence of strong shock in the region owing to reflection of shocks from the wall. The reflection of shock (strong) tends to travel downstream until subsidized by another reflected shock. The trend continues over the rest of the isolator axial length.

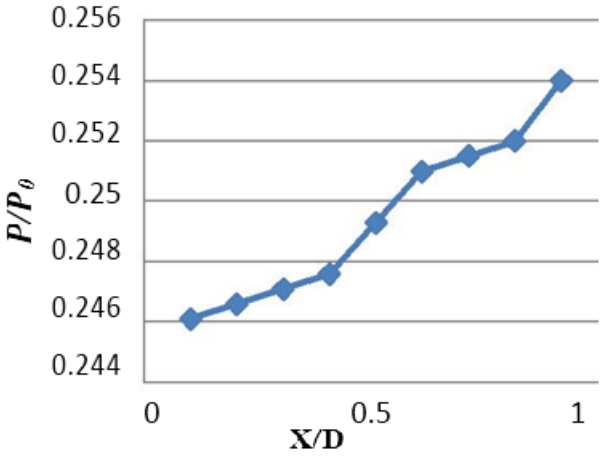

Fig. 4: Isolator wall pressure for 4 bar settling chamber pressure

For 500 kPa setup and at X/D = 0.2, the static pressure value is 0.1998 for P_0, due to weak shock structure. At X/D = 0.3, the wall static pressure to total pressure value 0.202 may be due to weak shock prevailing in the flow field. At X/D = 0.4 onwards up to exit of isolator, there is sudden rise in pressure due to the strong shock existence in the flow flied. For 600 kPa setup and at X/D = 0.1, the wall pressure varies up to 0.167 of total pressure due to weak nature of shock. Up to X/D = 0.8, the wall pressure increases drastically to a value of 0.182 for P_0.

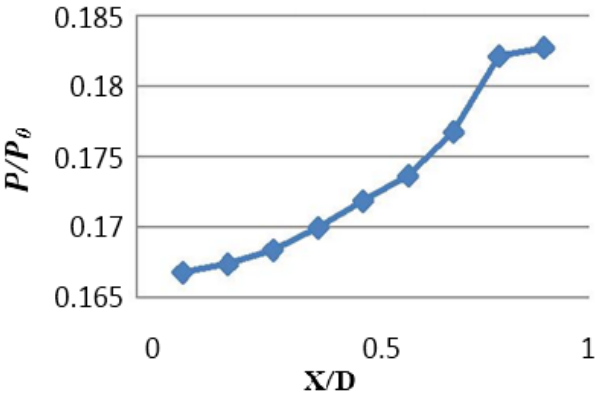

Fig. 5: Isolator wall pressure for 5 bar settling chamber pressure

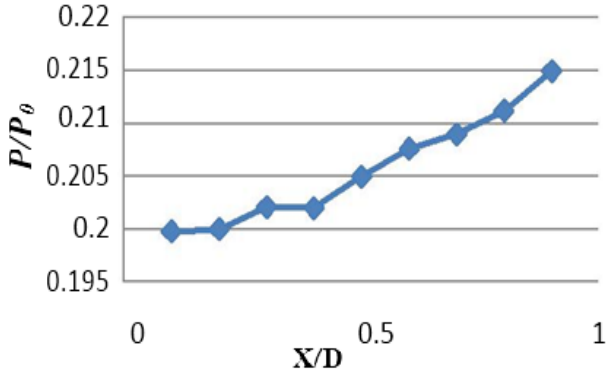

Fig. 6: Isolator wall pressure for 6 bar settling chamber pressure

For the hexagon shaped exit, Figs. 7 to 9 show the variation of P/P_0 over X/D for total pressure of 400 kPa, 500 kPa and 600 kPa respectively. For 400 kPa and at X/D = 0.1, the wall static pressure varies up to 0.25 of total pressure due to the presence of strong shock in the region. Up to X/D = 0.5, the wall pressure increases to a value of 0.2513 for P_0. The pressure rise is linear owing to weak nature of shock. At X/D = 0.5 onwards up to X/D = 0.7, the wall static pressure to total pressure values increased from 0.2513 to 0.2539. The pressure rises suddenly due to strong shock formation in the region. From X/D = 0.8 onwards up to exit of isolator, the pressure value increases and then decreases due to interaction of shocks. For 500 kPa, the shock is increasing uniformly from 0.199 to 0.21 at X/D = 0.2 to X/D = 0.3. From X/D = 0.3 to X/D = 0.6, the slope of wall pressure is increased uniform due to the presence of mild shock. From X/D = 0.5 to X/D = 0.7, the value of P/P_0 is 0.203 to 0.212 respectively which clearly demonstrates that the pressure increase is steeper due to decaying in velocity and flow field is accompanied by strong shock train.

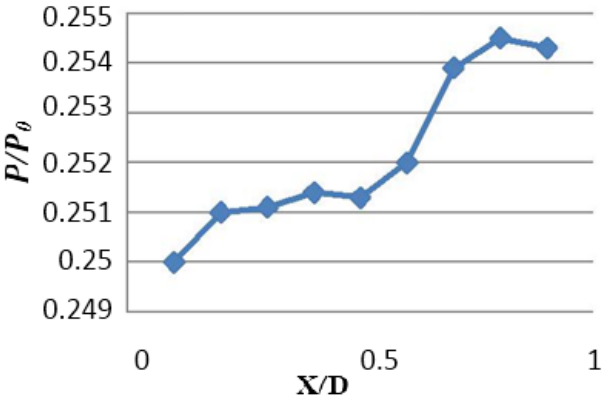

Fig. 7: Isolator wall pressure for 4 bar settling chamber pressure

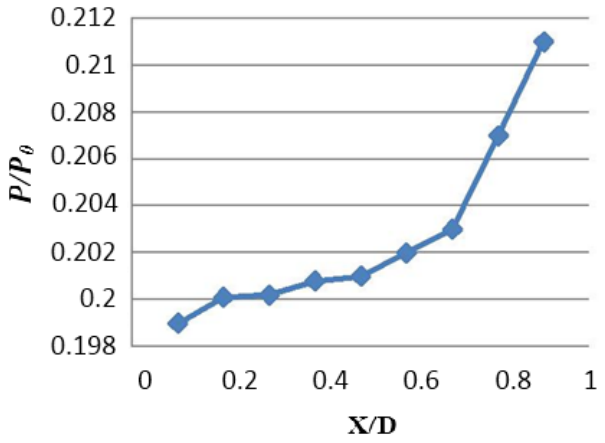

Fig. 8: Isolator wall pressure for 5 bar settling chamber pressure

For 600 kPa and at X/D = 0.1, the isolator pressure ratio increases with uniform inlet total pressure up to X/D = 0.3. The slope of the curve is steep for total pressure ratio 0.168 onwards up to 0.178. This reduction is due to presence of mixed shocks. Based on the experimental results presented, it can be conclude that the isolator pressure ratio increases with decreasing inlet total pressure. The increased pressure ratio is balanced by longer shock trains. The increase in shock train length is evident from the movement of sudden pressure rise position upstream with increasing pressure ratio. The slope of the curve is steep for total pressure greater than 400 kPa and the slope reduces for shock train length lesser than X/D = 0.6 i.e. for total pressure less than 400 kPa. This reduction is due to presence of mixed flow region with greater shock train length. This is evident from the plots as the slope of the curve levels after a sudden rise for higher pressure ratios.

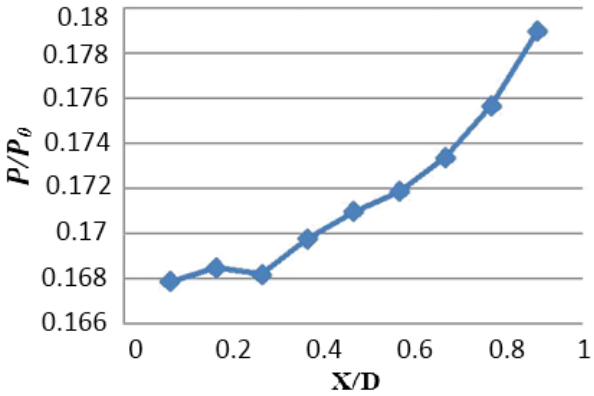

Fig. 9: Isolator wall pressure for 4 bar settling chamber pressure

4. Conclusion

The experimental investigations were carried over the experimental set-up of different transformation shaped cross sectional isolator configuration. The investigations were conducted experimentally under different isolator pressure ratios. The shock train lengths were found to increase for an increase in the isolator pressure ratios. Hence, the required isolator length for designed isolator pressure ratio can be reduced in case of high momentum flows. At higher pressure ratios, the subsonic flow is dominant compared to supersonic flow near the isolator exit and the subsonic flow withstands the imposed back pressure in major proportion.

The pressure ratio near the wall plane suggested that strong flow separation caused by initial shock in the shock train posing a substantial recirculation region. The recirculation together with the low momentum flow from the re-attachment of shock interaction with side walls brought together by geometry corner. This has acted as the mechanism in creation of vortex structures that travels in the stream wise direction known as corner vortices [4]. The pentagonal shape gives better performance than hexagonal shape. In pentagonal shape, the pressure rise is higher and hence the shock strength is stronger. When the shock is stronger, the pressure raise has resulted in reduction of Mach number and velocity. So, the shock is sustained by the isolator.

REFERENCES:

[1] A.C. Idris, M.R. Saad, H.Z. Behtash and K. Kontis. 2014. Luminescent measurement systems for the investigation of a scramjet inlet-isolator, *Sensors*, 14(4), 6606-6632. https://doi.org/10.3390/s140406606.

[2] A.M. Siddiqui and G.M.S. Ahmed. 2013. Design and analysis on scramjet engine inlet, *Int. J. Scientific and Research Publications*, 3(1), 1-12.

[3] C. Xuebin and Z. Kunyuan. 2010. Experimental investigation of the short isolator with the ramp under asymmetric incoming flow, *Proc. 46th AIAA/ASME/SAE/ Joint Propulsion Conf. & Exhibition*, Nashville, USA.

[4] W.E. Eagle, J.A. Benek and J.F. Driscoll. 2011. Experimental investigation of corner flows in rectangular supersonic inlets with 3D shock-boundary layer effects, *Proc. 49th AIAA Aerospace Sciences Meeting*, Orlando, USA. https://doi.org/10.2514/6.2011-857.

[5] H. Sugiyama, K. Fukuda, K. Mizobata, L. Sun and R. Minato. 2003. Experimental investigation on shock wave and turbulent boundary layer interactions in square duct at Mach 2 and 4, *Proc. Int. Gas Turbine Congress*, Tokyo, Japan.